

Baryon Electromagnetic Form Factors at BESIII

Isabella Garzia^{*†}

University of Ferrara and INFN-Sezione di Ferrara

E-mail: garzia@fe.infn.it

Electromagnetic form factors are fundamental observables needed to parametrize the electric and magnetic structure of hadrons and used to probe strong interactions. In this contribution we report on the recent measurements of baryon electromagnetic form factors at the BESIII experiment in Beijing. The BESIII spectrometer is located at the BEPCII collider, a symmetric e^+e^- collider running at the center-of-mass energies between 2.0 and 4.6 GeV. This wide energy range allows direct measurement of electromagnetic form factors both from direct e^+e^- annihilation and from initial-state-radiation processes. Based on the data collected by BESIII at twelve center-of-mass energies between 2.23 and 3.67 GeV, the $e^+e^- \rightarrow p\bar{p}$ cross section and the time-like proton form factors are measured. Preliminary results from the analysis on the initial-state-radiation radiation process $e^+e^- \rightarrow p\bar{p}\gamma$ using a data set of about 7.4 fb^{-1} collected at the center-of-mass energies between 3.773 and 4.6 GeV are also presented. Besides nucleons, all hyperons in the SU(3) spin 1/2 octet and spin 3/2 decuplet are energetically accessible within the BEPCII energy range. Furthermore, a world-leading data sample was collected in 2014-2015 for precision measurements of baryon form factors, which allows the measurement of the relative phase between the electric and magnetic form factors for Λ and Λ_c hyperons with unprecedented accuracy. The results from the $e^+e^- \rightarrow \Lambda\bar{\Lambda}$ and the $e^+e^- \rightarrow \Lambda_c\bar{\Lambda}_c$ channels are also discussed.

*23rd International Spin Physics Symposium - SPIN2018 -
10-14 September, 2018
Ferrara, Italy*

^{*}Speaker.

[†]On behalf of the BESIII Collaboration

1. Introduction

The confinement of quarks inside the hadrons is one of the most challenging question in contemporary physics. In particular, nucleons offer the ideal environment to study the strong interaction between the quarks. However, despite the huge efforts in the last years aimed at investigating the nucleons properties, they remain a puzzle. We neither understand their mass nor the spin: the current quarks only constitute about 1% of the total nucleon mass (mass generation problem) and about 33% of its spin (spin crisis). Due to the non-perturbative nature of such effects, theoretical predictions are not feasible and experimental results play a central role in the understanding. Important insights about the quarks distribution into the nucleons can be obtained by studying the electromagnetic structure.

Electromagnetic form factors (FFs) describe the modifications of the point-like photon-hadron vertex due to the structure of the hadrons. They provide information on the intrinsic electric and magnetic distributions of hadrons. In e^+e^- annihilation processes we can access to the so called Time-Like (TL) electromagnetic FFs. The number of FFs involved is related to the spin of the hadrons taken into account: the structure of a non point-like particle of spin S is parametrized in terms of $(2S + 1)$ FFs. Considering the production of a spin 1/2 baryon-antibaryon pair $e^+e^- \rightarrow B\bar{B}$, where the baryon can be either a nucleon or a hyperon, and assuming that one-photon exchange $e^+e^- \rightarrow \gamma^* \rightarrow B\bar{B}$ is the dominant process, the differential cross section can be parametrized in terms of electric and magnetic FFs G_E and G_M , respectively. The Born differential cross section in the e^+e^- center-of-mass (c.m.) system is written as [1]:

$$\frac{d\sigma^{Born}(q^2, \theta_B)}{d\Omega} = \frac{\alpha^2 \beta C}{4q^2} \left[(1 + \cos^2 \theta_B) |G_M(q^2)|^2 + \frac{1}{\tau} \sin^2 \theta_B |G_E(q^2)|^2 \right], \quad (1.1)$$

where q is the momentum transfer, $\alpha \sim 1/137$ is the fine structure constant, θ_B is the polar angle of the baryon, $\tau = q^2/4m_B$ with m_B being the mass of the baryon, and $\beta = \sqrt{1 - 1/\tau}$. The Coulomb factor $C = y/(1 - \exp(-y))$, with $y = \pi\alpha/\beta$, accounts for the electromagnetic $B\bar{B}$ interactions of point-like baryons [2], and is equal to one for neutral baryon pairs. The integration of the differential cross section over the full solid angle Ω leads to the total Born cross section:

$$\sigma^{Born}(q^2) = \frac{4\pi\alpha^2\beta C}{3q^2} \left[|G_M(q^2)|^2 + \frac{1}{2\tau} |G_E(q^2)|^2 \right]. \quad (1.2)$$

An effective form factor (EFF) can be defined as:

$$|G(q^2)|^2 = \frac{2\tau |G_M(q^2)|^2 + |G_E(q^2)|^2}{2\tau + 1} = \frac{\sigma^{Born}(q^2)}{\left(1 + \frac{1}{2\tau}\right) \left(\frac{4\pi\alpha^2\beta C}{3q^2}\right)}, \quad (1.3)$$

which is equivalent to $|G_M(q^2)|$ under the working hypothesis $|G_M(q^2)| = |G_E(q^2)|$. It is often convenient to describe the production in terms of the EFF and the ratio $R = |G_E(q^2)|/|G_M(q^2)|$ between the electric and the magnetic FF at a given q^2 . The ratio R is extracted from the angular distributions of the outgoing baryons.

TL electromagnetic FFs are complex functions of the momentum transfer with a relative phase $\Delta\Phi$. This phase induces polarization effects in the final state. Since strong and electromagnetic interactions conserve parity, the polarization of the baryon in $e^+e^- \rightarrow B\bar{B}$ process must be perpendicular to the production plane spanned by the incoming beam and the outgoing baryon or antibaryon.

The polarization P depends on the phase and the scattering angle of the baryon as [3]:

$$P_n = -\frac{\sin 2\theta_B/\sqrt{\tau}}{(1 + \cos^2 \theta_B) + \frac{R^2}{\tau}(1 - \cos^2 \theta_B)} R \sin \Delta\Phi. \quad (1.4)$$

Therefore, $\Delta\Phi$ and the module of the phase can be extracted from the baryon polarization measurements. Hyperons have an advantage with respect to the nucleons in the sense that they decay weakly. The interference of the decay amplitudes in the hyperon decay causes the daughter baryon to be emitted in the direction of the mother hyperon. Thus the polarization of the hyperons is accessible via the angular distribution of their decay products, as well as the spin correlation of the outgoing hyperon and antihyperon.

An alternative approach to measure hadronic cross section at high luminosity e^+e^- storage ring is the study of initial-state-radiation (ISR), in which one or several photons are radiated from the initial state. The differential cross section for ISR process $e^+e^- \rightarrow B\bar{B}\gamma$ is related to the cross section of the non-radiative process through

$$\frac{d^2\sigma^{ISR}}{dq^2 d\theta_\gamma} = \frac{1}{s} W(s, x, \theta_\gamma) \cdot \sigma^{Born}(q^2), \quad (1.5)$$

where $x = 2E_\gamma/\sqrt{20}$, E_γ and θ_γ are the energy and the polar angle of the ISR photon in the e^+e^- c.m., respectively, and \sqrt{s} is the c.m. energy of the collider. The radiator function $W(s, x, \theta_\gamma)$ describes the probability of the ISR photon emission [4]. The emission of the ISR photon leads to a reduction of the invariant mass of the final state (q^2), and hence allows the measurement of the electromagnetic FFs over a wide range of q^2 below \sqrt{s} .

2. The BESIII experiment

The measurements are performed using data collected by Beijing Spectrometer (BESIII) [5] at the Beijing Electron-Positron Collider BEPCII. BEPCII is a double-ring symmetric collider optimized to work in the τ -charm energy region, with \sqrt{s} from 2.0 to 4.6 GeV. BESIII is a cylindrical detector which covers 93% of the full solid angle, and it consists of several sub-detectors. A small-celled, helium-based main drift chamber (MDC) which provides momentum measurements of charged particles with a resolution of 0.5% at 1 GeV/ c in a 1 T magnetic field. It also provides a measurement of the energy loss dE/dx with a resolution better than 6% for electrons from Bhabha scattering. A time-of-flight plastic scintillator (TOF) consisting of 5 cm thick plastic scintillator with a time resolution of 80 (110) ps in the barrel (end caps), corresponding to a $2\sigma K/\pi$ separation for momenta up to about 1.0 GeV/ c . A CsI(Tl) Electromagnetic Calorimeter (EMC) consisting of 6240 crystals in a cylindrical structure and two end caps, used to measure the energies of photons and electrons. Its energy resolution for 1 GeV photon can reach 2.5% (5%) in the barrel (end caps). Finally, a Muon Chamber (MUC) consisting of 1000 m² of resistive plate chambers is used to identify muons and it provides a spatial resolution better than 2 cm. More details can be found in [5].

BESIII provided the world's largest samples of e^+e^- collision in the τ -charm region, and it will continue to collect data up to 2024. Data samples have been collected at different charmonium and X, Y, Z states, and high luminosity scan data have been accumulated in the region between 2.0

and 4.6 GeV. These data allow the measurement of baryon FFs using both direct e^+e^- annihilation and ISR radiation processes.

3. Proton FFs at BESIII

The study of the process $e^+e^- \rightarrow p\bar{p}$ with two different techniques, energy scan and ISR, allows a complementary approach to the measurement of the Born cross section and proton FFs. The first technique provides very accurate measurements at well defined energies, while ISR allows a continuous measurement over a wide range of momentum transfer. Below, we report the results obtained by BESIII through the use of both techniques.

3.1 Study of the $e^+e^- \rightarrow p\bar{p}$ processes using energy scan technique

The cross section for the process $e^+e^- \rightarrow p\bar{p}$ at 12 c.m. energies between 2.2 and 3.7 GeV was measured by BESIII using a data sample of 157 pb^{-1} collected during 2011 and 2012 data taking [6]. The Born cross section is calculated by

$$\sigma_{Born} = \frac{N_{obs} - N_{bkg}}{\mathcal{L}\varepsilon(1 + \delta)}, \quad (3.1)$$

where N_{obs} is the number of observed events, N_{bkg} is the number of background events, \mathcal{L} is the integrated luminosity which is determined at each \sqrt{s} , ε is the detection efficiency, and $(1 + \delta)$ is the radiative correction factor up to the next-leading-order calculated by means of the CONEX event generator [7]. The corresponding EFF of the proton is then obtained from Eq. (1.3). The obtained Borns cross section and EFF are shown in Figure 1, in which also the comparison with previous experimental measurements is shown.

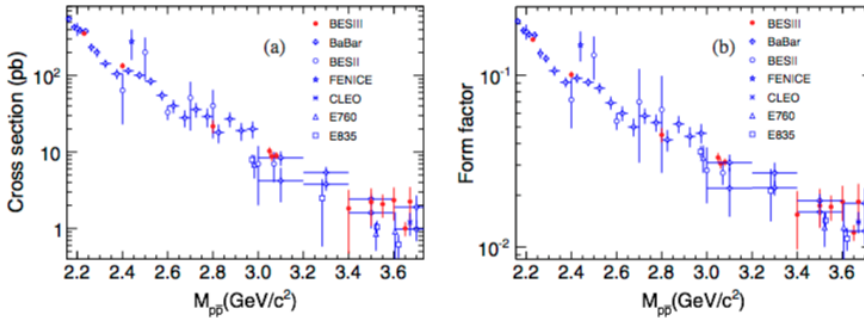


Figure 1: Comparison of (a) the Born cross section and (b) the EFF between BESIII (red points) and previous measurements [6].

An improvement of about 30% was achieved on Born cross section measurements below $\sqrt{s} = 3.08 \text{ GeV}$. The ratio of the proton FFs is extracted from the fit to the distribution of the proton polar angle using the larger data samples (see Table 1); it is found to be close to unity in agreement with BaBar results [8] in the same q^2 region.

\sqrt{s} (GeV)	$ G_E/G_M $
2.2324	$0.87 \pm 0.24 \pm 0.05$
2.4000	$0.91 \pm 0.38 \pm 0.12$
3.0500 and 3.0800	$0.95 \pm 0.45 \pm 0.21$

Table 1: Results for the ratio $R = |G_E/G_M|$ from [6].

3.2 Study of the $e^+e^- \rightarrow p\bar{p}$ processes using ISR technique

Based on a sample of 7.408 fb^{-1} data collected at \sqrt{s} between 3.773 and 4.600 GeV at BESIII, the proton FFs have been measured by studying of the ISR process $e^+e^- \rightarrow p\bar{p}\gamma$. Two kind of scenarios can be distinguished depending on whether the radiative photon can be detected (large angle (LA) or tagged photon, about 12% of events) or not detected (small angle (SA) or undetected photon, about 46% of events).

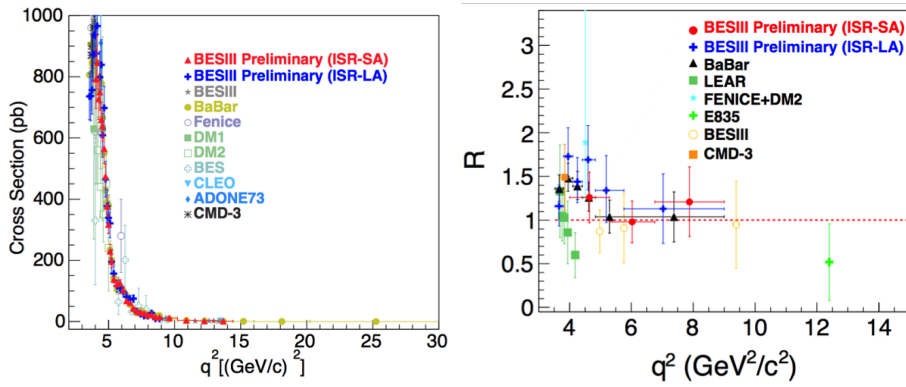


Figure 2: BESIII preliminary results on the Born cross section (left plot) and preliminary results on the ratio of the proton FFs (right plot) from ISR measurement of $e^+e^- \rightarrow p\bar{p}\gamma$ process.

The ratio R has been extracted for six different bins of the $p\bar{p}$ invariant mass from the production threshold up to $3.0 \text{ GeV}/c^2$. The Born cross section and the proton EFF have been also measured in 31 intervals of $p\bar{p}$ -invariant mass below $3.0 \text{ GeV}/c^2$ for the LA analysis, while 30 intervals of $p\bar{p}$ -invariant mass below $3.8 \text{ GeV}/c^2$ are used for the SA analysis. Preliminary results are available for both scenarios, which are shown in Figure 2. They are consistent with previous experiments. The total uncertainty, dominated by the statistical one, is between 20% and 35% for the ratio, and between 5% and 64% for the Born cross section.

4. Hyperon Form Factors: measurement of $e^+e^- \rightarrow \Lambda\bar{\Lambda}$

BESIII recently published results on the measurement of the $e^+e^- \rightarrow \Lambda\bar{\Lambda}$ cross section and EFF [9]. The analysis was based on 40.5 pb^{-1} of data collected at four different energy scan points during 2011 and 2012. The lowest energy point is only 1 MeV above the $\Lambda\bar{\Lambda}$ threshold, which allows to study the Born cross section behavior almost at threshold. In order to increase the statistics, both events where the Λ and $\bar{\Lambda}$ decay to charged mode ($\Lambda \rightarrow p\pi^-$ and $\bar{\Lambda} \rightarrow \bar{p}\pi^+$), and events where the $\bar{\Lambda}$ decays to the neutral mode ($\bar{\Lambda} \rightarrow \bar{n}\pi^0$) were selected. Details on event

and track selection can be found in [9]. The Born cross section and EFF are shown in Figure 3 and compared with previous measurements [10, 11]. These results are in good agreement with those from BaBar [10], and they improve the measurement of at least 10% at low momentum transfer, and even more above 2.4 GeV/ c . The Born cross section at threshold is found to be $305 \pm$

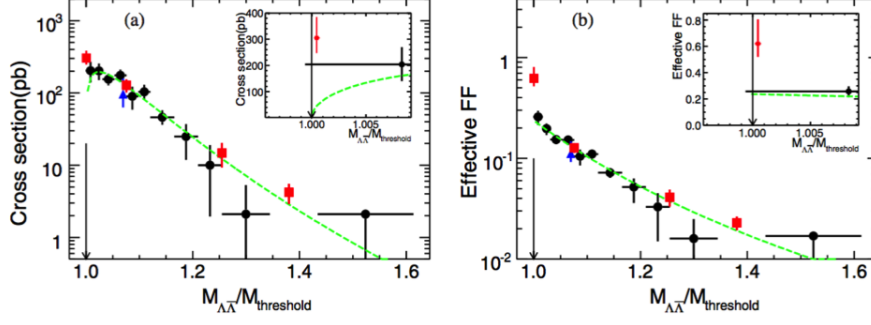


Figure 3: Measurement of $e^+e^- \rightarrow \Lambda\bar{\Lambda}$ cross section (left plot) and Λ EFF (right plot).

45_{-36}^{+66} pb, where the first and second uncertainty refer to the statistical and systematic uncertainties, respectively. Given that the Coulomb factor in Eq. (1.2) is equal to 1 for neutral baryon pairs, the cross section is expected to go to zero at threshold. The observed threshold enhancement implies a more complicated physics scenario that requires more theoretical investigations [12]. It was also interpreted as an attractive Coulomb interaction on the constituent quark level [13].

In a very recent preliminary BESIII result, we report for the first time the observation of spin polarization of Λ and $\bar{\Lambda}$ hyperons from the coherent production in the $J/\psi \rightarrow \Lambda\bar{\Lambda}$ process by means of a sample of 1.31×10^9 J/ψ events [14]. The Λ ($\bar{\Lambda}$) hyperon decays via a parity non-conserving weak process, and its polarization is extracted from the angular distribution of its decay products. A clear polarization is observed and the results summarized in Figure 4, where the moment $\mu(\cos\theta_\Lambda)$ is directly related to the polarization: $\mu(\cos\theta_\Lambda) \sim \sqrt{1 - \alpha_\psi^2} \alpha_- \sin\Delta\Phi \cos\theta_\Lambda \sin\theta_\Lambda$. Therefore,

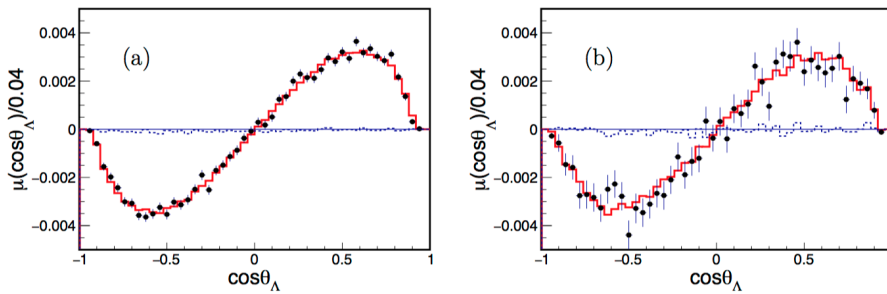


Figure 4: Moments $\mu(\cos\theta_\Lambda)$ for acceptance uncorrected data as a function of $\cos\theta_\Lambda$ for (a) $p\pi^-\bar{p}\pi^+$ and $p\pi^-\bar{n}\pi^0$ events. Points with error bars refer to data, solid histogram is the global fit result, and the dashed histogram show the expected result in the no polarization scenario [14].

the phase $\Delta\Phi = \Phi_E - \Phi_M$ is determined to be $(42.4 \pm 0.6 \pm 0.5)^\circ$, where the first uncertainty is statistical and the second systematic. It agrees and improves preliminary BESIII results at $\sqrt{s} = 2.396$ GeV. The angular distribution parameter α_ψ and the asymmetry parameters α_- , α_+ , and $\bar{\alpha}_0$

for the $\Lambda \rightarrow p\pi^-$, $\bar{\Lambda} \rightarrow \bar{p}\pi^+$, and $\bar{\Lambda} \rightarrow \bar{n}\pi^0$ decays, respectively, are also extracted. In particular, the value of $\alpha_- = 0.750 \pm 0.009 \pm 0.004$ differs by more than five standard deviations from the value quoted by the Particle Data Group [15]. This means that all the published measurements on the $\Lambda/\bar{\Lambda}$ polarization are larger than $\sim 17\%$.

5. Measurement of $e^+e^- \rightarrow \Lambda_c \bar{\Lambda}_c$ close to the production threshold

BESIII has pushed the results on the measurement of the channel $e^+e^- \rightarrow \Lambda_c^+ \bar{\Lambda}_c^-$ [16]. The analysis was based on a sample of 631.3 pb^{-1} data collected at four different scan energy points in 2014: $\sqrt{s} = 4.5745, 4.5809, 4.5900, \text{ and } 4.5995 \text{ GeV}$. The lowest energy point is only 1.6 MeV above the $\Lambda_c^+ \bar{\Lambda}_c^-$ threshold. At each decay mode, ten Cabibbo-favored hadronic decay modes are used to reconstruct Λ_c^+ or $\bar{\Lambda}_c^-$. The Born cross section for the i -th mode is calculated as:

$$\sigma_i = \frac{N_i}{\varepsilon_i \mathcal{L} f_{VP} \text{BR}_i f_{ISR}}, \quad (5.1)$$

where N_i and ε_i represent the yield and the corresponding detection efficiency, \mathcal{L} is the integrated luminosity, f_{VP} is the vacuum polarization correction factor, BR_i represents the branching ratio product of the i -th decay mode, and f_{ISR} is the ISR correction factor. Then, the total cross section is obtained by weighted average over the individual measurements. The results are shown in Figure 5. A rise of the cross section in proximity of the threshold is observed, which is an indication of the complexity of the Λ_c production behavior.

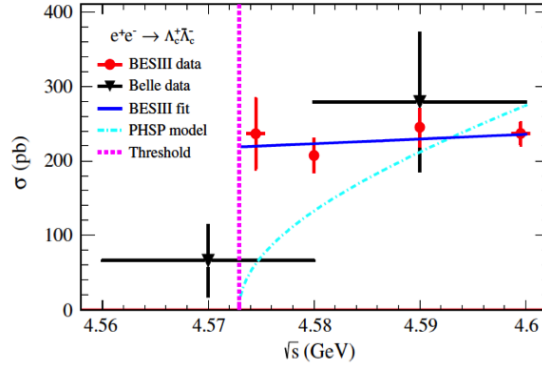


Figure 5: Cross section of $e^+e^- \rightarrow \Lambda_c \bar{\Lambda}_c$ obtained by BESIII [16] and Belle [17]. The blue solid curve represents the input-line shape in the generator when determining f_{ISR} . The dash-dotted cyan curve denotes the prediction of the phase-space model (Eq. (1.2)) with $C = 1$ and flat $|G_M|$ with respect to \sqrt{s} .

The higher statistic data samples $\sqrt{s} = 4.5745$ and 4.5995 GeV are used to study the polar angle distribution of Λ_c in the e^+e^- c.m. system, and to extract the ratio $|G_E/G_M|$ for the first time. The polar angle distribution is fitted with the function $f(\theta) \propto (1 + \alpha_{\Lambda_c} \cos^2 \theta)$, and the $|G_E/G_M|$ ratio extracted using:

$$|G_E/G_M|(1 - \beta^2) = (1 - \alpha_{\Lambda_c})/(1 + \alpha_{\Lambda_c}). \quad (5.2)$$

The results, summarized in Table 2, provide important insights into the production mechanism and structure of Λ_c baryons. In a future extension of this analysis, also the polarization and the spin

correlation of the outgoing Λ_c pair can be extracted, making possible the full determination of the Λ_c electromagnetic FFs.

\sqrt{s} (GeV)	α_{Λ_c}	$ G_E/G_M $
4.5745	$-0.13 \pm 0.12 \pm 0.08$	$1.14 \pm 0.14 \pm 0.07$
4.5995	$-0.20 \pm 0.04 \pm 0.02$	$1.23 \pm 0.05 \pm 0.03$

Table 2: Shape parameters of the angular distribution and $|G_E/G_M|$ ratio [16]. The uncertainty are statistical and systematic, respectively.

6. Summary and prospects

The experimental measurements of the TL baryon FFs close to the threshold region show some unexpected features [18, 19], and a precise and complete measurement of the FFs in this region is of great importance. BESIII is an excellent laboratory for baryon FFs studies, since both scan energy and ISR methods can be exploit and the kinematical threshold of different baryon production are covered. The proton electromagnetic FFs have been studied with very high precision and studies of the neutron FFs are ongoing. Measurements of the Λ and Λ_c FFs has been published, and for the first time a preliminary result on the relative phase between $|G_E|$ and $|G_M|$ of Λ FFs is obtained. New results on other hyperons FFs will be available soon.

References

- [1] A. Zichichi, S. M. Berman, N. Cabibbo and R. Gatto, *NuovoCimento* **24** 170 (1962).
- [2] C. Tzara, *Nucl.Phys. B* **18** 216-252 (1970).
- [3] A. Z. Dubnickova et al., *NuovoCimento A* **109**, 241 (1996).
- [4] G. Bonneau and F. Martin, *Nucl.Phys. B* **27** 381 (1971).
- [5] M. Ablikim et al., *Nucl.Instrum.Meth. A* **614**, 345 (2010).
- [6] M. Ablikim et al., *Phys. Rev. D* **91**, 112004 (2015).
- [7] R. G. Ping, *Chin. Phys. C* **38**, 083001 (2014).
- [8] J. P. Lees et al. (BABAR Collaboration), *Phys. Rev. D* **87**, 092005 (2013); *Phys. Rev. D* **88**, 072009 (2013).
- [9] M. Ablikim et al., *Phys. Rev. D* **97**, 032013 (2018).
- [10] B. Aubert et al., *Phys. Rev. D* **76**, 092006 (2007).
- [11] D. Bisello et al., *Z. Phys. C* **48**, 23 (1990).
- [12] O.D.Dalkarov, P.A.Khakhulinand and A.Y.Voronin, *Nucl. Phys. A* **833**,103(2010); B.El-Bennich, M. Lacombe, B. Loiseau and S. Wycech, *Phys.Rev. C* **79**, 054001 (2009); J. Haidenbauer, H.-W. Hammer, U. G. Meißner and A. Sibirtsev, *Phys. Lett. B* **643**, 29 (2006); H. Fonvieille and V. A. Karmanov, *Eur. Phys. J. A* **42**, 287 (2009).
- [13] R. Baldini, S. Pacetti, A. Zallo and A. Zichichi, *Eur. Phys. J. A* **39**, 315 (2009).

- [14] M. Ablikim et al., arXiv:1808.08917.
- [15] M. Tanabashi et al., Phys. Rev. D **98**, 030001 (2018).
- [16] M. Ablikim et al., Phys. Rev. Lett. **120**, 132001 (2018).
- [17] G. Pakhlova et al., Phys. Rev. Lett. **101**, 172001 (2008).
- [18] A. Bianconi and E. Tomesi-Gustafsson, Phys. Rev. C **93**, 035201 (2016).
- [19] J. Haidenbauer and U. G. Meissner, Phys. Lett. B **761**, 456 (2016).